

Supplementary Information

Engineering the structure of ZIF-derived catalysts by revealing the critical role of temperature for enhanced oxygen reduction reaction

Zelin Wang¹, Xiaoxing Ke^{1,*}, Kailing Zhou², Xiaolong Xu³, Yuhong Jin², Hao
Wang², and Manling Sui^{1,*}

1. Beijing Key Laboratory of Microstructure and Properties of Solids, Faculty of
Materials and Manufacturing, Beijing University of Technology, Beijing 100124, China;
2. College of Materials Science, Faculty of Materials and Manufacturing, Beijing
University of Technology, Beijing 100124, China
3. School of Materials Science and Engineering, Qilu University of Technology
(Shandong Academy of Sciences), Jinan 250353, China

Corresponding authors:

Xiaoxing Ke, Email: kexiaoxing@bjut.edu.cn, ORCID: 0000-0003-2004-6906;

Manling Sui, Email: mlsui@bjut.edu.cn, ORCID: 0000-0002-0415-5881

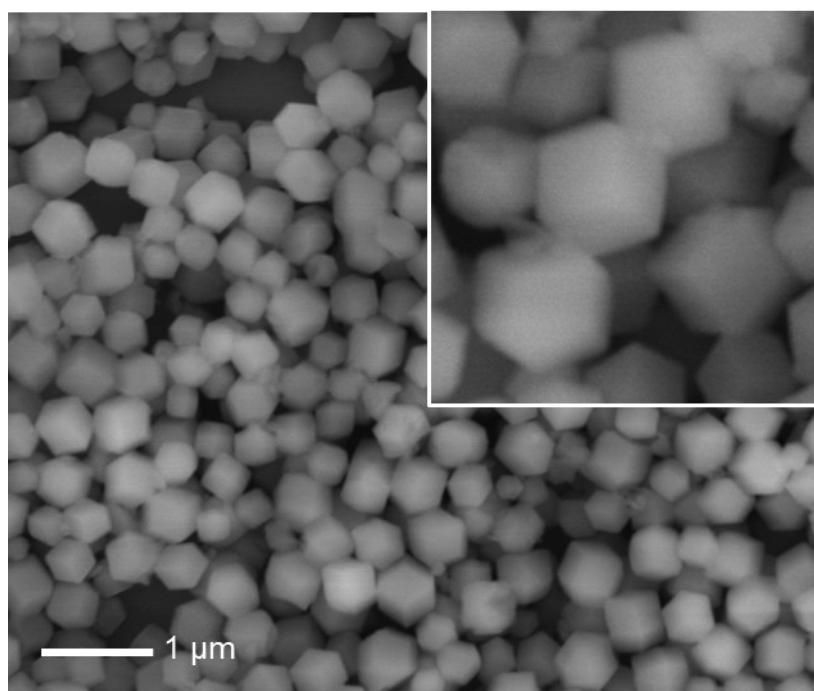


Figure S1. SEM image of as-synthesized ZIF-67 particles and enlarged as inset.

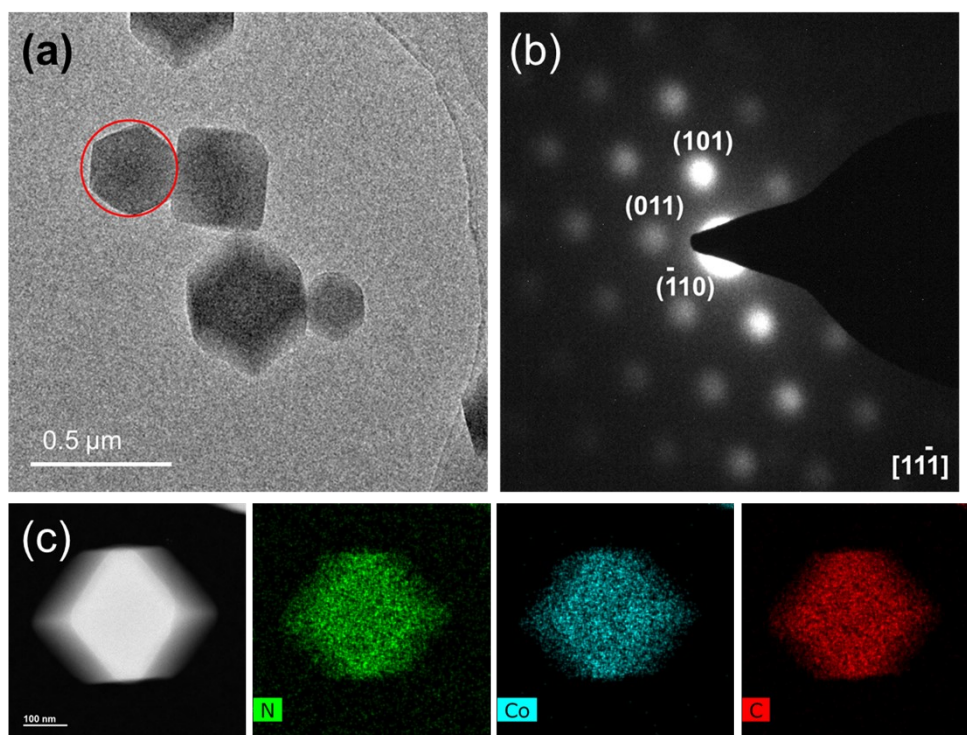


Figure S2. (a) TEM image of as-synthesized ZIF-67. Due to beam-sensitivity of ZIF-67 structure, limited dose rate of $<1 \text{ e}\text{\AA}^{-2}\cdot\text{s}^{-1}$ is used for image acquisition. (b) SAED pattern of circled area in (a). (c) Corresponding EDS mapping of N, Co and C, respectively.

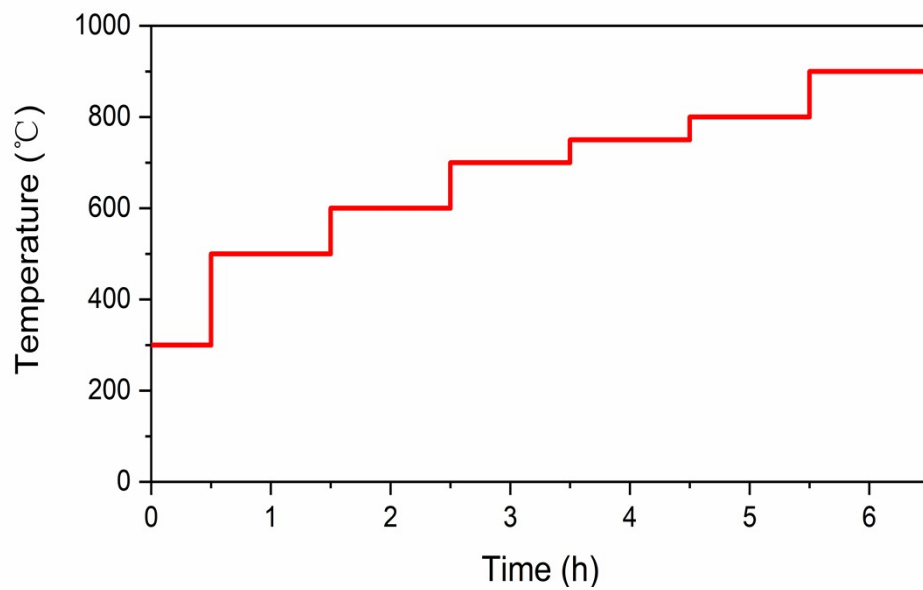


Figure S3. Illustration of annealing setup (temperature vs time) for *in-situ* experiments.

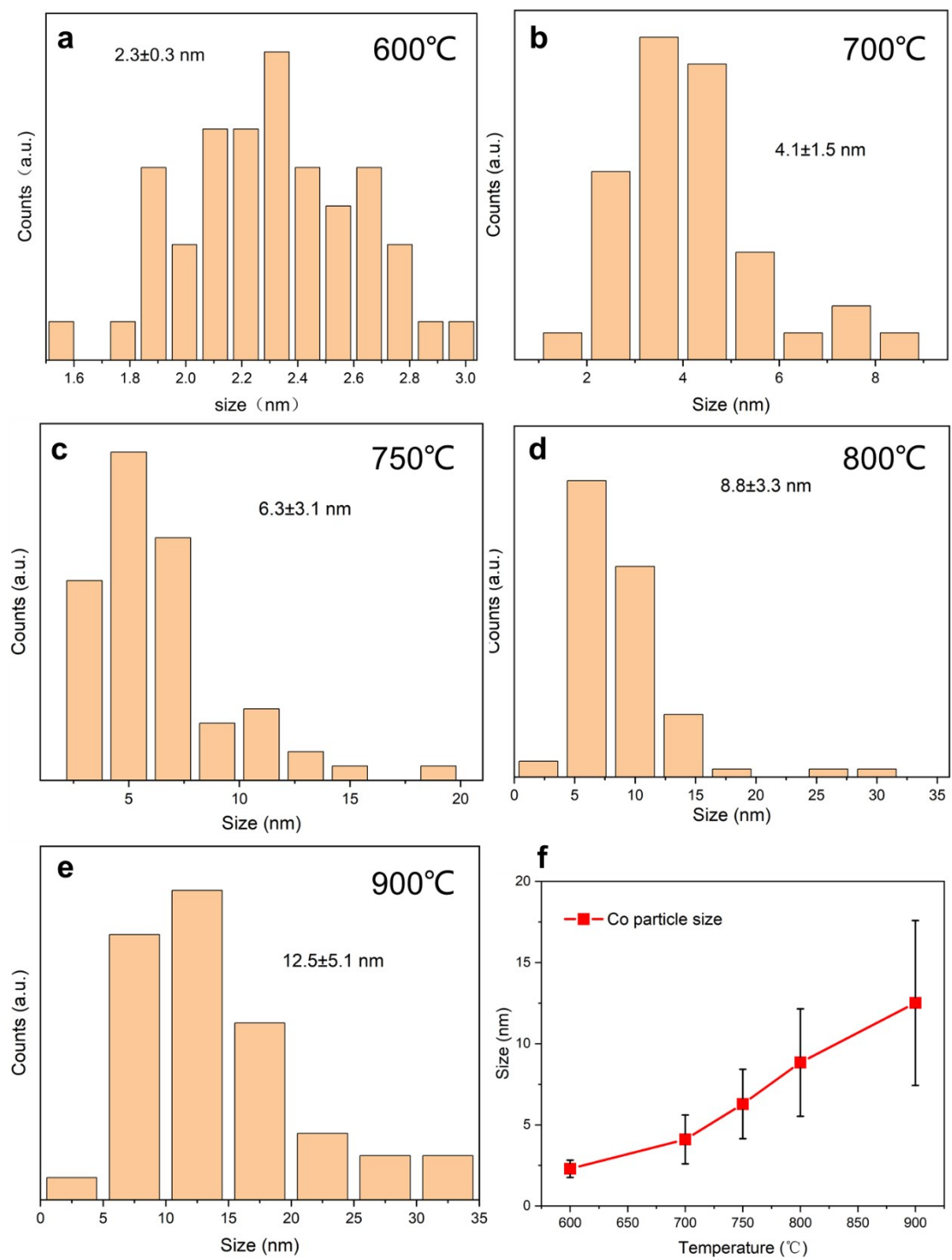


Figure S4. Size distributions of Co nanoparticles embedded in ZIF-67 pyrolyzed at (a) 600°C, (b) 700°C, (c) 750°C, (d) 800°C, (e) 900°C, and (f) summarizing chart.

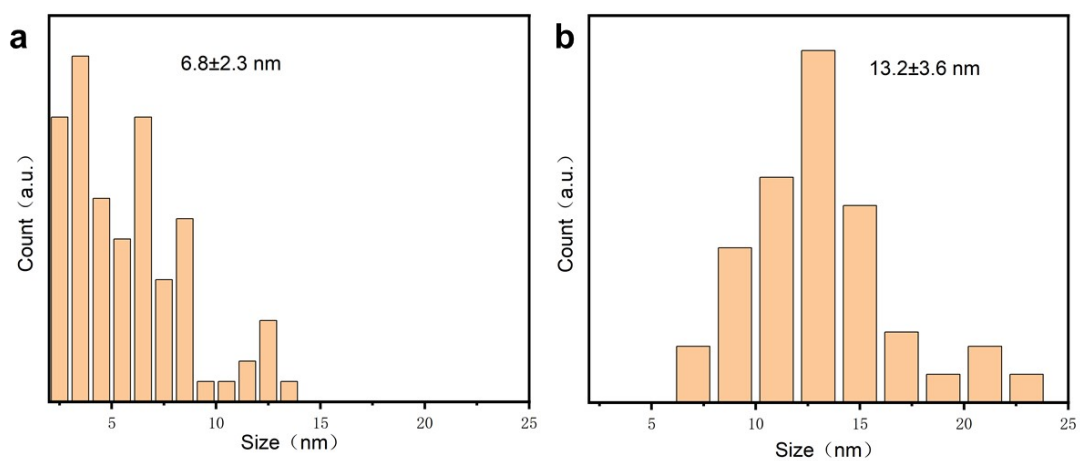


Figure S5. Pore size distributions of ZIF-67 pyrolyzed at (a) 750°C and (b) 900°C.

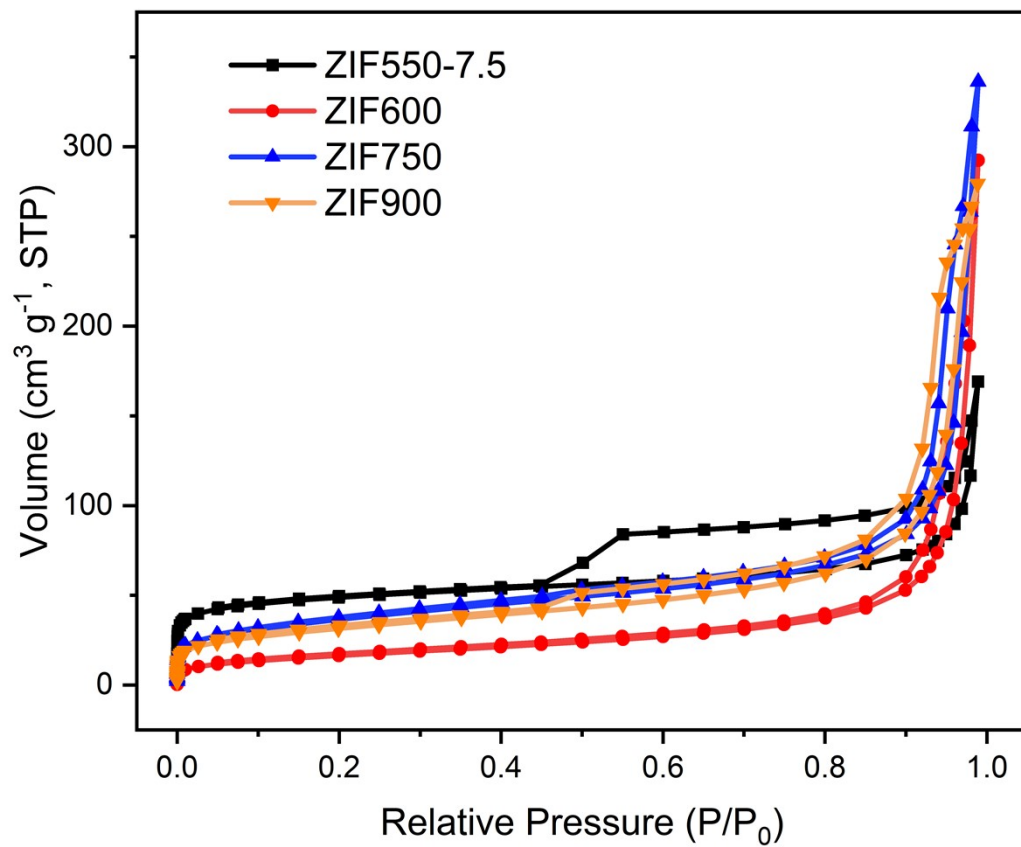


Fig. S6. N₂ adsorption-desorption isotherms of ZIF600, ZIF750, ZIF900 and ZIF550-7.5h.

Table. S1. BET surface area and average pore size of ZIF600, ZIF750, ZIF900, and ZIF550-7.5h.

Sample	S_{BET} (m²g⁻¹)	Average pore diameter (nm)
ZIF600	59.6	
ZIF750	129.7	15.5
ZIF900	111.9	16.1
ZIF550-7.5h	187.0	5.8

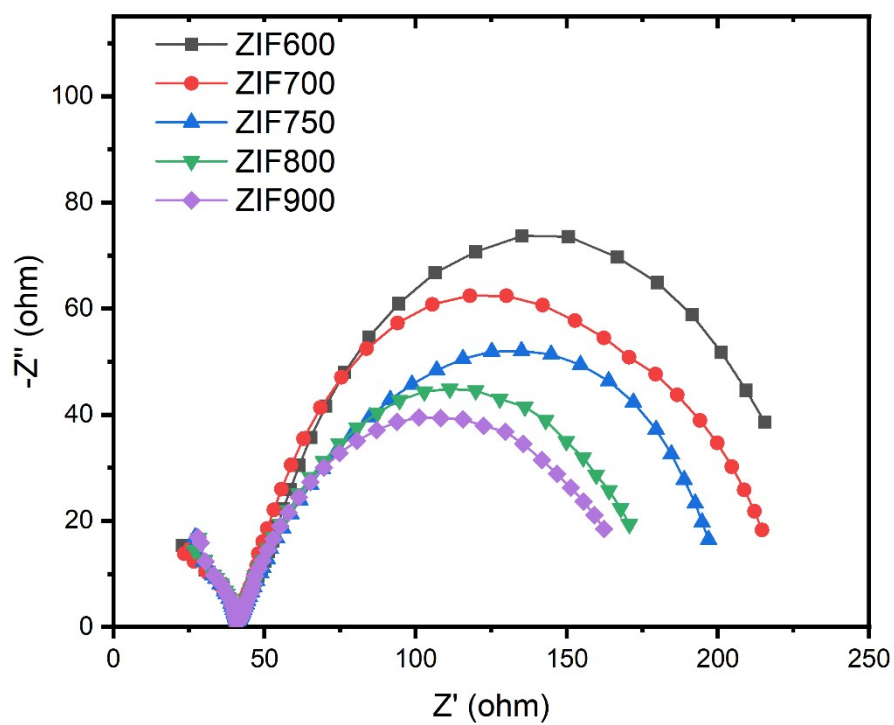


Figure S7. EIS Nyquist plots of ZIF600, ZIF700, ZIF750, ZIF800 and ZIF900.

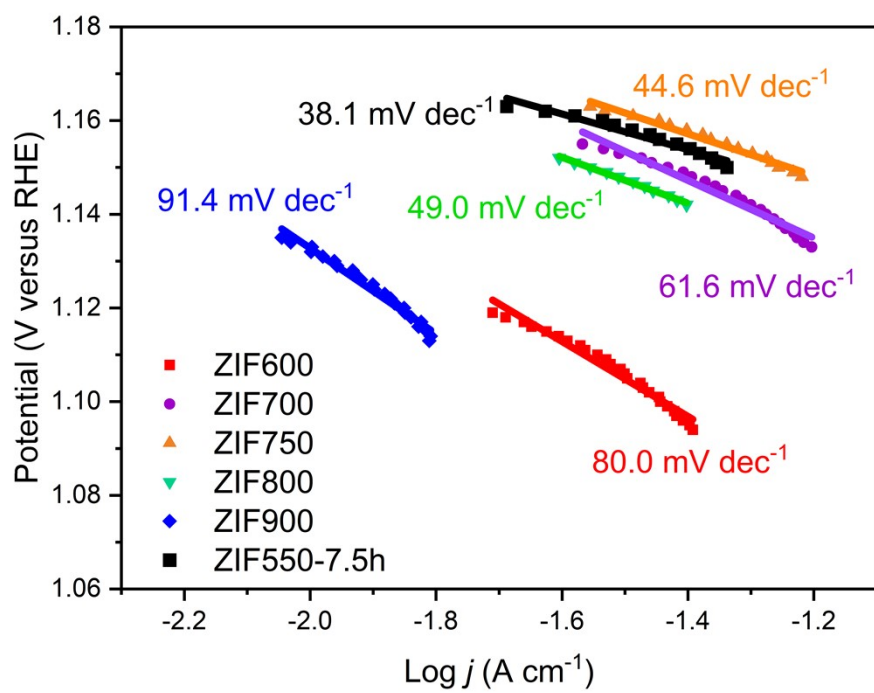


Fig. S8. Tafel slopes of ZIF600, ZIF700, ZIF750, ZIF800, ZIF900, and ZIF550-7.5h.

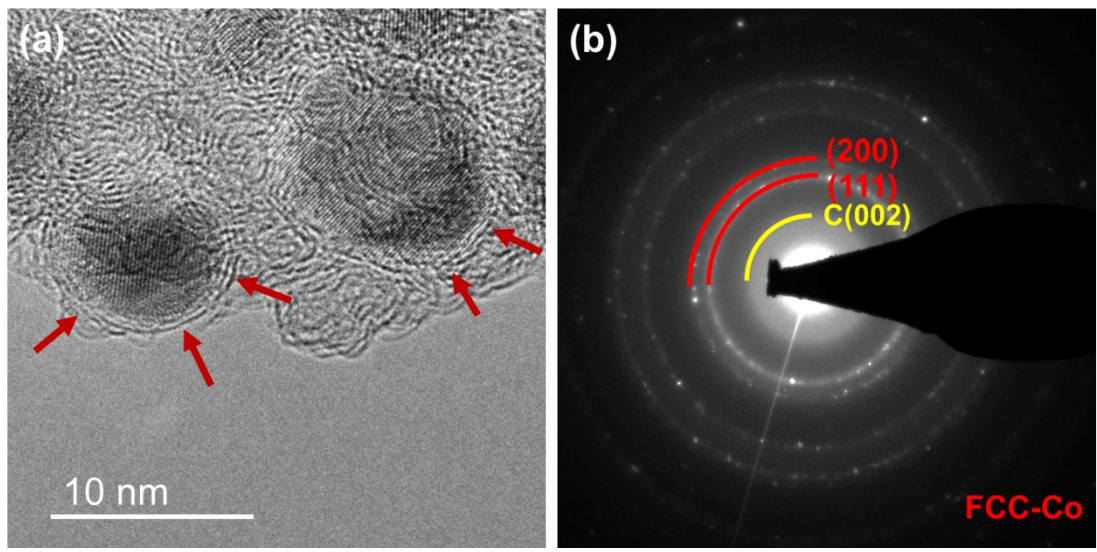


Figure S9. (a) TEM image and (b) corresponding SAED pattern of ZIF750. Arrows indicate few-layer-graphene wrapping.

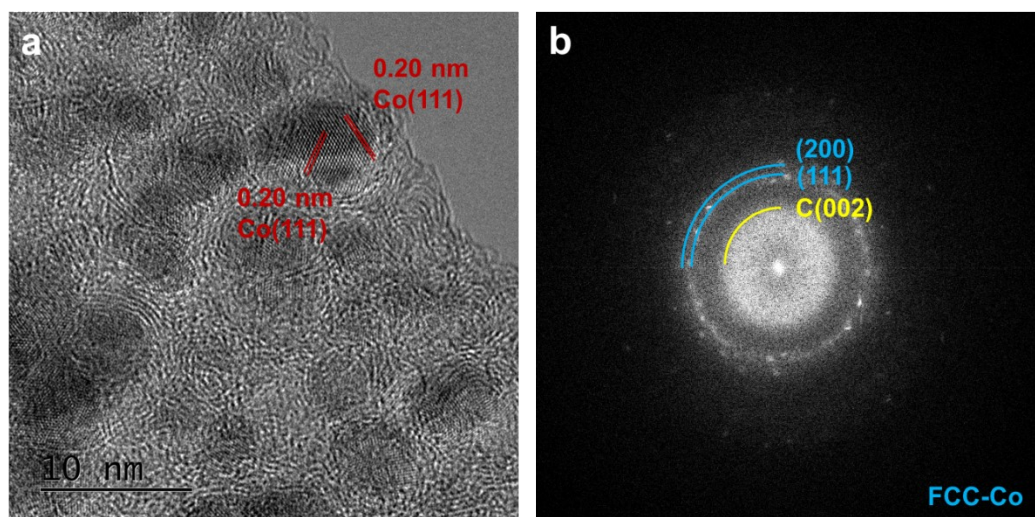


Fig. S10. (a) TEM image and (b) corresponding FFT pattern of ZIF-750 after duration test.

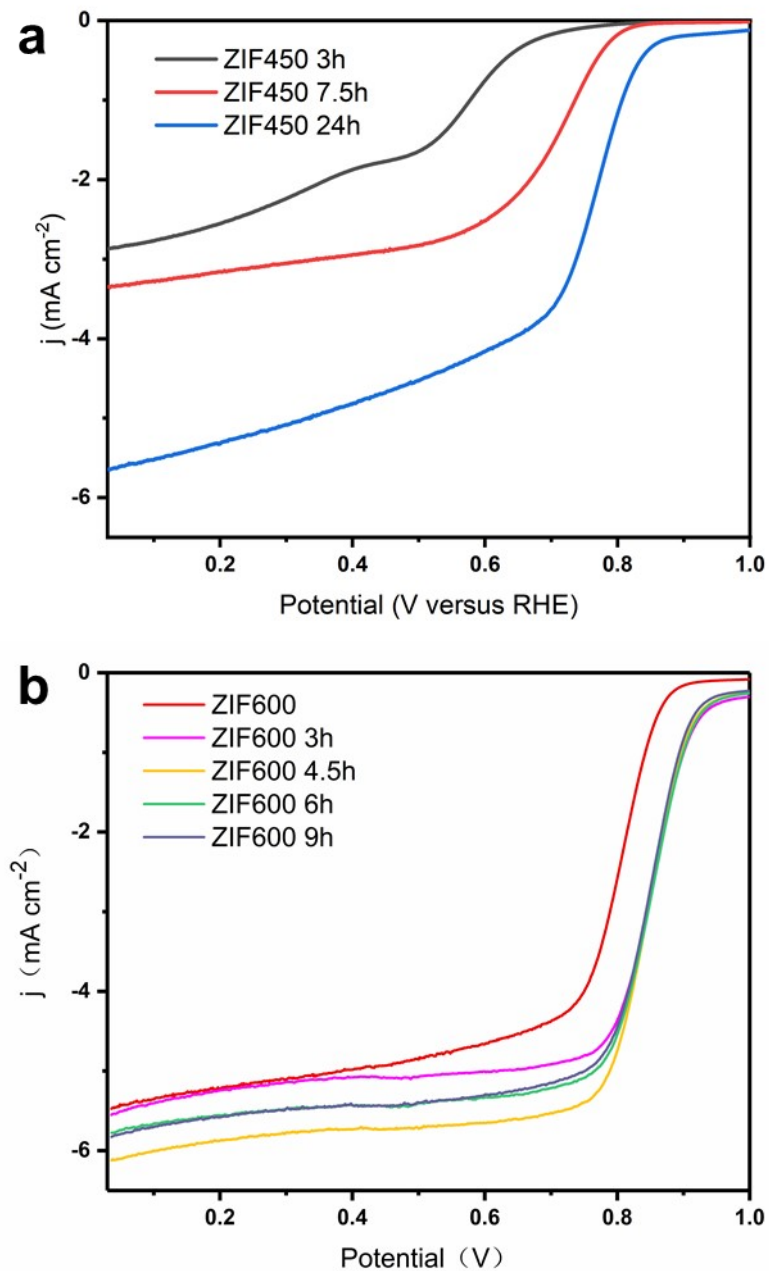


Figure S11. Steady-state polarization ORR plots in O₂-saturated 0.1 M KOH at rotation rate of 1600 rpm with a scan rate of 5 mV s⁻¹ for (a) ZIF450-3h, ZIF450-7.5h, ZIF450-24h and (b) ZIF600, ZIF600-3h, ZIF600-4.5h, ZIF600-6h, ZIF600-9h.

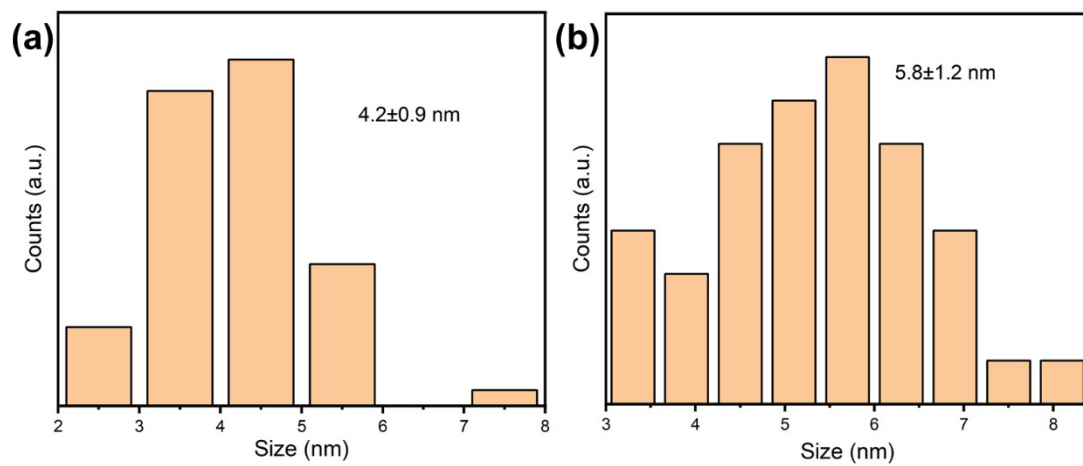
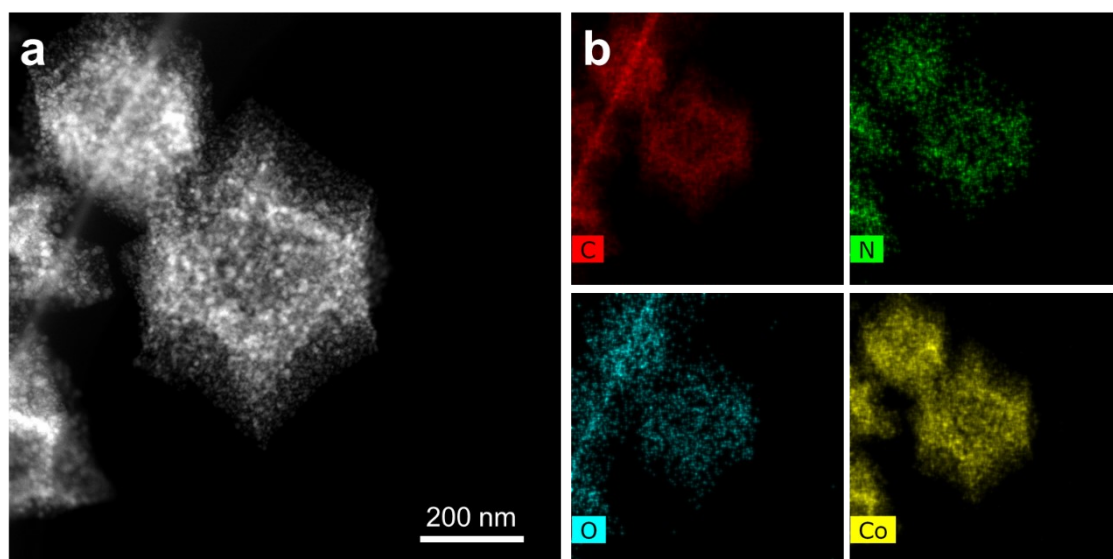


Figure S12. (a) Co nanoparticle size distribution and (b) Pore size distributions of ZIF550-7.5h.



c

Element	C	N	O	Co
wt%	67.9	5.5	2.3	24.3

Figure S13. (a) HAADF-STEM images of ZIF550-7.5h. (b) EDS mapping of C, N, O and Co, respectively. (c) Corresponding EDS quantification results.

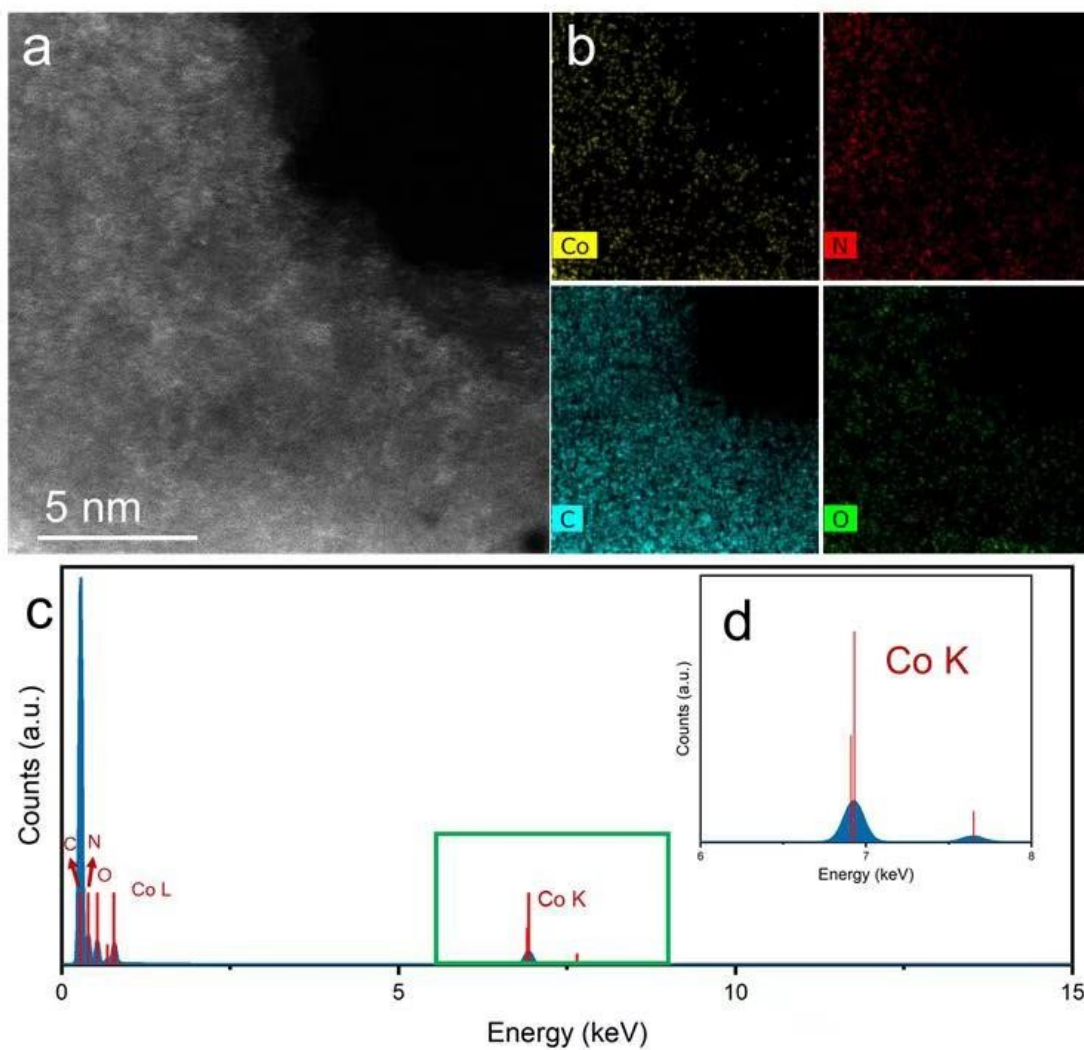


Figure S14. (a) HAADF-STEM image of an area without Co nanoparticles but with Co single atoms in ZIF550-7.5h. (b) EDS mapping of Co, N, C, O in (a). (c) Corresponding EDX spectrum and (d) enlargement from boxed area.

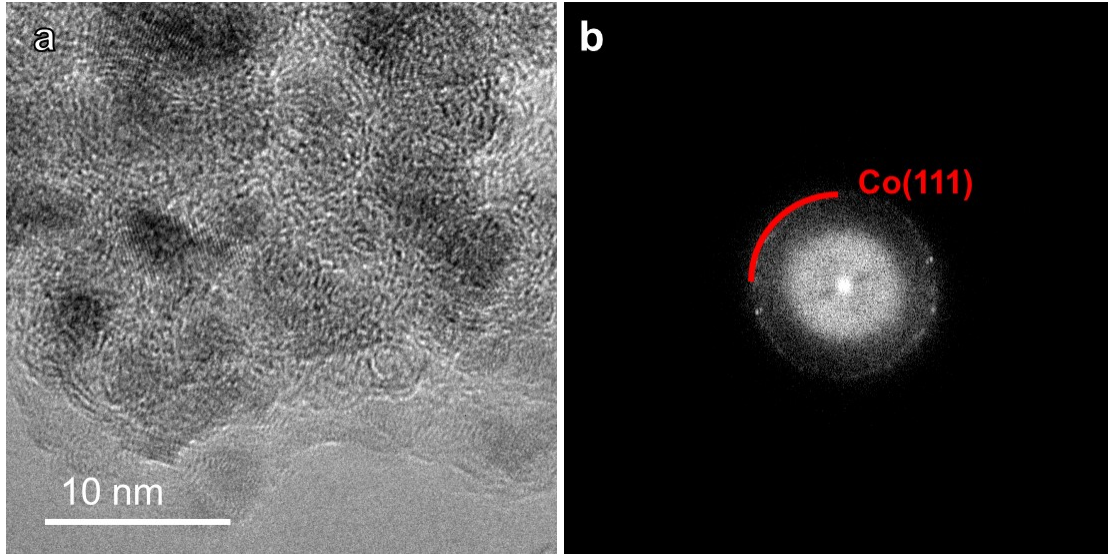


Figure S15. (a) TEM image and (b) corresponding FFT image of ZIF450-24h.

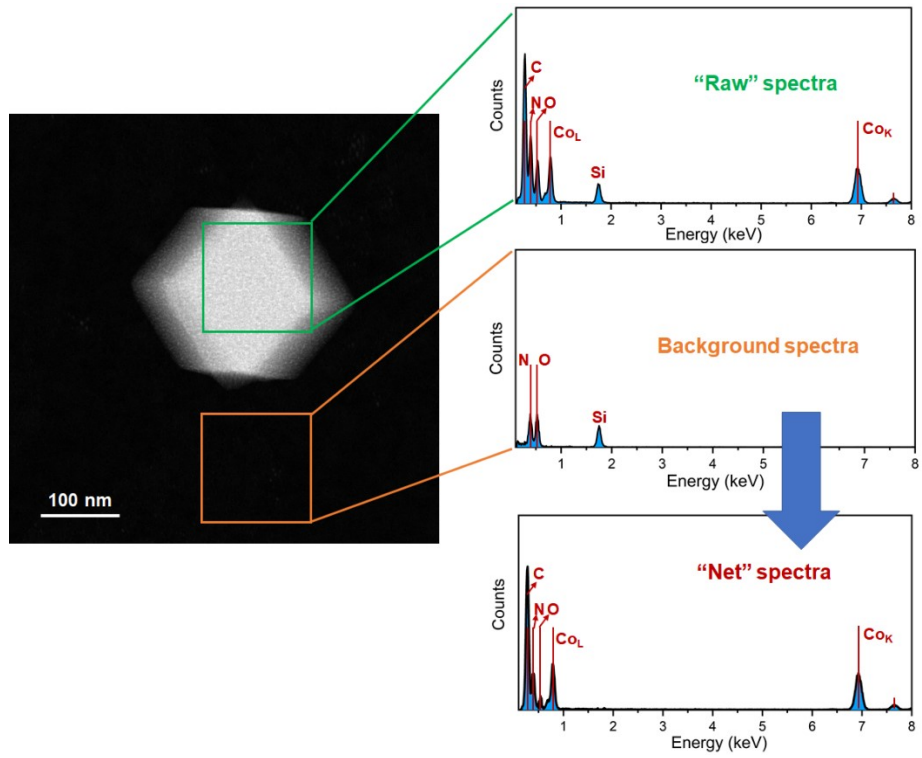


Fig. S16. Experimental procedure of nitrogen quantification where the influence of nitrogen from SiN thin film is excluded.